JACS
JOURNAL OF THE AMERICAN CHEMICAL SOCIETY

Communication

pubs.acs.org/JACS

# Physical Organic Approach to Persistent, Cyclable, Low-Potential Electrolytes for Flow Battery Applications

Christo S. Sevov,[†,‡] David P. Hickey,[†,§] Monique E. Cook,[†,‡] Sophia G. Robinson,[†,§] Shoshanna Barnett,[†,‡] Shelley D. Minteer,[*,†,§] Matthew S. Sigman,[*,†,§] and Melanie S. Sanford[*,†,‡]

[†]Joint Center for Energy Storage Research, 9700 S. Cass Avenue, Argonne, Illinois 60439, United States
[‡]Department of Chemistry, University of Michigan, 930 N. University Avenue, Ann Arbor, Michigan 48109, United States
[§]Department of Chemistry, University of Utah, 315 South 1400 East, Salt Lake City, Utah 84112, United States

Supporting Information

**ABSTRACT:** The deployment of nonaqueous redox flow batteries for grid-scale energy storage has been impeded by a lack of electrolytes that undergo redox events at as low (anolyte) or high (catholyte) potentials as possible while exhibiting the stability and cycling lifetimes necessary for a battery device. Herein, we report a new approach to electrolyte design that uses physical organic tools for the predictive targeting of electrolytes that possess this combination of properties. We apply this approach to the identification of a new pyridinium-based anolyte that undergoes 1$e^-$ electrochemical charge−discharge cycling at low potential (−1.21 V vs Fc/Fc$^+$) to a 95% state-of-charge without detectable capacity loss after 200 cycles.

Redox-flow batteries (RFBs) offer a potential solution to the unmet challenge of the large-scale integration of intermittent renewable energy sources into the electrical grid.[1] In an RFB, solvated anolyte and catholyte molecules are pumped over inert electrodes to charge/discharge the battery and are then stored in separate reservoirs. This design principle means that RFBs can be inexpensively scaled by simply adding more of the electroactive compounds to the external reservoirs.[2] Techno-economic modeling has implicated redox-active organic molecules (ROMs) as particularly attractive electrolytes for RFBs due to their relatively low cost and molecular weights, as well as the feasibility of achieving high solubility and significant electrochemical potential differences between the anolyte and catholyte.[3] However, even if all of these techno-economic metrics are met, ROM-based electrolytes will not be viable unless they are long-lived in both the charged and discharged states and undergo stable electrochemical cycling.

Many ROMs, particularly those that store considerable amounts of energy by undergoing redox reactions at low (anolytes) or high (catholytes) potentials, have poor shelf-lives in the charged state and undergo fast decomposition during charge−discharge cycling.[4] To date, no general strategies have been developed for improving/optimizing the lifetime (herein referred to as persistence) and cyclability of ROMs without concomitantly decreasing their redox potential window.[4f,5] Herein, we introduce a physical organic approach to designing persistent organic electrolytes that undergo stable cycling in acetonitrile at low potentials.

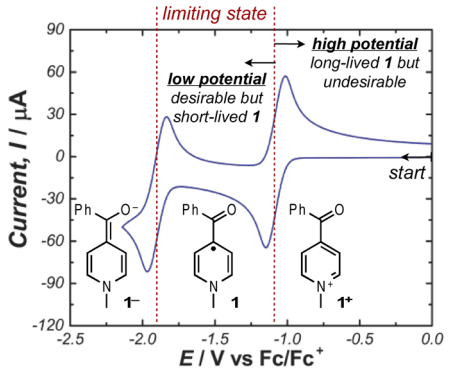


**Figure 1.** CV of $\mathbf{1}^+$ (0.1 M $TBAPF_6$ in $CH_3CN$ at 100 mV/s).

We selected anolyte candidate $\mathbf{1}^+$ as a test case for our design strategy. A recent report demonstrated that this acylpyridinium derivative meets a number of techno-economic metrics for nonaqueous RFB applications, including high solubility (1.5 M in acetonitrile), low molecular weight per electron transferred (142 g/mol of $e^-$), and multiple redox events at relatively low potentials [−1.08 and −1.78 V vs Fc/Fc$^+$ (Fc = ferrocene), Figure 1].[6] However, the application of this molecule in nonaqueous RFBs remains fundamentally limited by the short lifetime of the radical **1**,[7] which is formed upon the 1$e^-$ reduction of $\mathbf{1}^+$. For example, 0.29 M solutions prepared from isolated samples of **1** decay by ∼7% over 24 h at room temperature; furthermore, ∼20% capacity fade is observed after just 75 charge−discharge cycles between $\mathbf{1}^+$ and **1**. We hypothesized that modeling tools based on physical organic parameters could be used to identify second generation anolytes with enhanced persistence while maintaining the low redox potential associated with the parent molecule. Notably, although such tools have been successfully applied in the fields of drug development,[8] catalyst design,[9] and mechanistic study,[10] they have not yet been utilized for the development of energy storage materials.

We implemented a five-step workflow to develop a quantitative correlation between the structures of 4-acylpyr-

**Received:** January 5, 2017




DOI: 10.1021/jacs.7b00147
J. Am. Chem. Soc. XXXX, XXX, XXX−XXX

idinium derivatives and their redox potentials and persistence.[9a,11] First, a training set of 12 acylpyridine radicals was synthesized, and the rate of decomposition was measured for each. Second, a set of physical-organic parameters was identified to relate the experimental decomposition rates to the electronic and steric properties of each molecule in the training set. Third, a mathematical relationship was established to identify the key structural and electronic features responsible for persistence. Fourth, virtual extrapolation of the mathematical model was used to predict new anolytes with improved properties.[10a] Finally, the predicted molecules were synthesized and validated, ultimately leading to new anolytes with dramatically enhanced persistence as well as lower redox potentials.

Radicals **1**−**12** were selected for the initial training set, because they represent a range of steric and electronic variation at different sites on the acylpyridinium core (Figure 2). The decomposition of each was monitored at 70 °C in $CD_3CN$ via NMR spectroscopy. As an example, a 0.30 M solution of **1** degraded through three half-lives in a 12 h period with a second order rate constant of $6.6 \times 10^{-4}$ $M^{-1}$ $s^{-1}$ (Figure 2, top).[12] A number of trends are apparent from the training set. For example, radicals bearing electron-donating substituents (e.g., **2**) generally have more negative potentials but also faster rates of decomposition than electron deficient analogues (e.g., **4**).

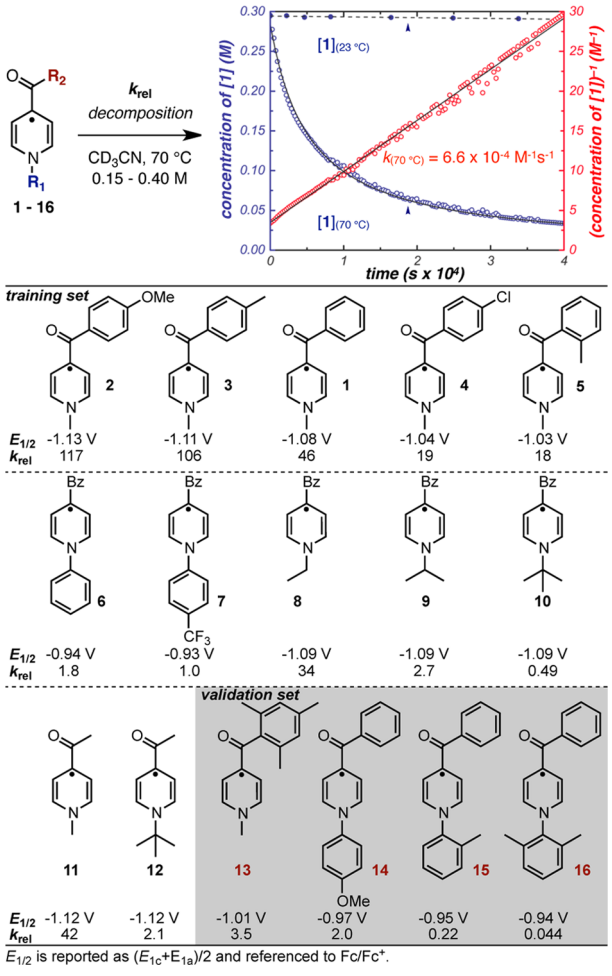


**Figure 2.** Decomposition studies of **1**−**16** in $CD_3CN$ at 70 °C. Plot of [**1**] (blue, left axis) and 1/[**1**] (red, right axis) vs time (top). Redox potentials and relative rates of decomposition of **1**−**16** (bottom).

Conversely, the less electron-rich *N*-aryl derivatives **6** and **7** exhibit enhanced lifetimes but more positive reduction potentials. These data are all consistent with a ground state electronic stabilization of the radical (which is reported to be localized at the 4-position of the pyridine)[13] by electron withdrawing substituents. Furthermore, they reinforce the general paradigm that persistence and potential are inversely correlated.[14] Although distal to the primary site of radical density, steric hindrance at nitrogen itself has been previously demonstrated to improve the persistence of related pyridine radicals.[15] Indeed, upon systematically increasing the size of the nitrogen substituent (**1**, **8**, **9**, **10**), we observe significant enhancements in radical persistence. For example, the *tert*-butyl-substituted benzoylpyridine **10** exhibits a 100-fold slower rate of decomposition relative to the *N*-methyl analogue **1**. In this case, the dramatic improvement in radical lifetime does not occur at the expense of potential, providing promising evidence that persistence and redox potential can be decoupled through the judicious modification of appropriate substituents.

We next focused on generating a predictive model for the virtual evaluation of new pyridinium anolytes. Using the data above, we calculated thermodynamic properties and identified computationally derived structural descriptors for the training set anolytes (Figure 3a). As substituent size appeared to be influential, initial correlations were attempted using a variety of traditional steric parameters (i.e., Charton and Sterimol).[9b] Poor trends were observed in all cases ($R^2 < 0.60$), prompting the examination of alternative descriptors. This ultimately led to the identification of a parameter describing the substituent height out of the pyridine ring plane ($H_{st}$). This effectively accounts for the combined steric effects of the substituents at nitrogen, at C2, and at C6. Using a linear regression algorithm

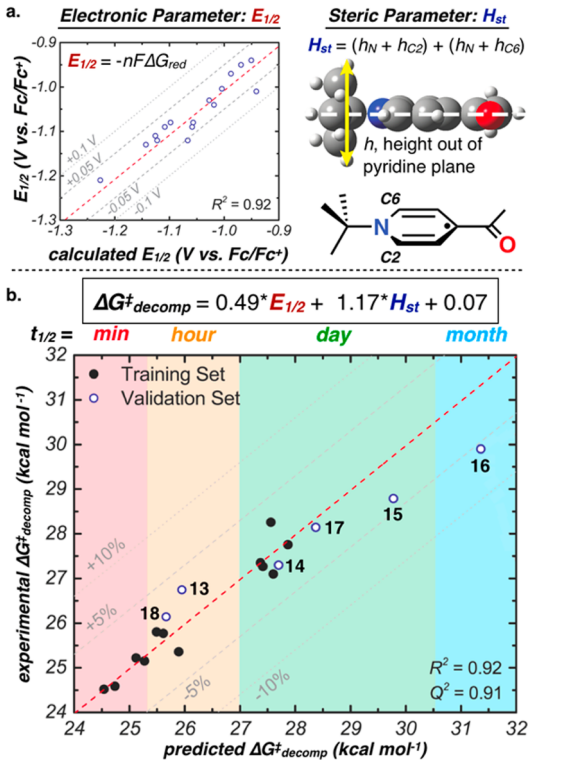


**Figure 3.** (a) Illustration of the electronic and steric descriptors. (b) Plot of predicted vs experimentally determined free energies for decomposition of training (●) set and validation (○) set.



DOI: 10.1021/jacs.7b00147
J. Am. Chem. Soc. XXXX, XXX, XXX−XXX

to explore a range of parameters, a statistical correlation ($R^2$ = 0.92) was found when $H_{st}$ was used in combination with computed electrochemical reduction potentials (Figure 3b). This simple relationship illustrates that reduction potential and radical persistence can indeed be decoupled via the incorporation of appropriate substituents at nitrogen, at C2, and/or at C6.

With a tool for quantitative prediction in hand, we next sought to test the extrapolative limits of the model by identifying a radical with exceptional persistence (defined for our purposes as $t_{1/2} \geq 1$ month at 70 °C). We conducted a directed virtual screen of 18 compounds, focusing on maximizing $\Delta G^{\ddagger}_{dec}$ according to the physical descriptors in the equation. This screen suggested that *N*-xylyl-substituted **16** should exhibit 3 orders of magnitude greater persistence than the parent radical **1** and should thus persist for months at 70 °C. Experimentally, we found that **16** exhibits such high persistence that it exceeds the capabilities of our standard protocol to experimentally measure a rate of decomposition, necessitating that measurements be performed over 1 week at 70 °C. This example highlights an extrapolation in rate constant of over an order of magnitude from the limit of the original training set, corresponding to 2.3 kcal/mol greater $\Delta G^{\ddagger}_{dec}$. To understand better the origin of the observed persistence, we obtained a single crystal X-ray structure of **16**. As illustrated in Figure 4a, the solid state structure of **16** shows that the perpendicular xylyl substituent protects the C2/C6 positions of the pyridine ring, which presumably slows the homocoupling of two pyridine radicals.[15a]

Consistent with the existing paradigm, the high persistence of anolyte **16** mainly results from a ground-state stabilization, which leads to an undesirably high reduction potential of −0.94 V vs $Fc/Fc^+$. However, the utility of our parameter-based modeling tool is that we can now rapidly identify compounds with high charged-state persistence without sacrificing low potential. As depicted in Figure 4, plotting the lifetimes of charged anolytes **1**−**16** as a function of their potential reveals a quadrant diagram with corners that represent combinations of high/low potential and high/low persistence. The most desirable anolytes reside in the upper left quadrant. Targeting this region, we virtually evaluated a variety of molecules that (i) are predicted to have enhanced redox potentials and persistence, (ii) have substituents that add minimal molecular weight, and (iii) are synthetically accessible.

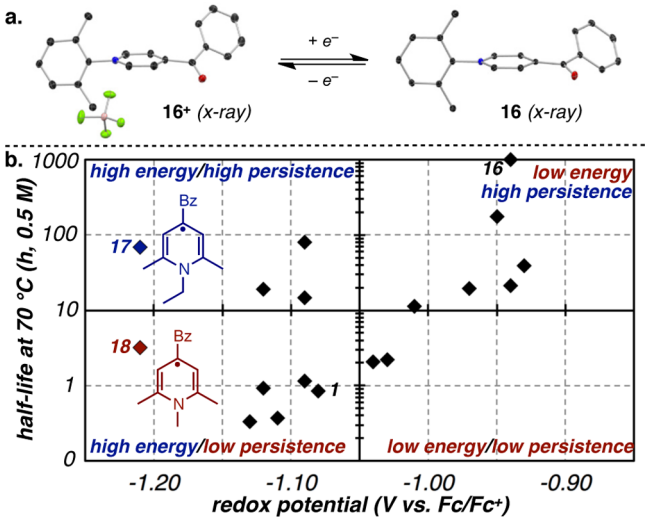


**Figure 4.** (a) X-ray structures of $\mathbf{16}^+$ and **16**. (b) Quadrant diagram of radical half-life as a function of redox potential.

Among the modeled anolyte candidates, **17** was selected for experimental testing, as it was predicted to exhibit high persistence as well as a potential lower than that of any derivative examined to date (predicted to be −1.23 V versus $Fc/Fc^+$, Figure 3a).[16] Compound **17** also incorporates the first examples of substituents at the C2 and C6 positions of the pyridine ring, thereby providing a key test of the extrapolative capabilities of the model. As predicted, **17** exhibits the lowest experimental potential (−1.21 V vs $Fc/Fc^+$) and one of the longest radical lifetimes ($k_{rel}$ = 0.56). The model's ability to predict accurately the decomposition barrier of **17** ($\Delta G^{\ddagger}_{pred}$ = 28.4 kcal/mol, $\Delta G^{\ddagger}_{exp}$ = 28.2 kcal/mol) represents an electronic extrapolation of nearly 100 mV beyond the training set, while simultaneously demonstrating its ability to account for a new substituent pattern.

Most important for the identification of desirable RFB electrolytes is that the model accounts for nonintuitive effects of chemical structure on persistence. For example, the *N*-methyl analog **18** was predicted and experimentally validated to exhibit an approximately 20-fold lower persistence than the *N*-ethyl anolyte **17**. This is in contrast to the *N*-methyl and *N*-ethyl derivatives **1** and **8**, respectively, which display nearly identical lifetimes. Because the reduction potentials for **17** and **18** are essentially the same, the ∼2 kcal/mol enhanced stability of **17** arises from a difference in kinetic stability, reflected by the parameter $H_{st}$ (Et = 9.06 Å vs Me = 5.16 Å). This appears to result from gearing between the Et group and the 2,6 substituents, which forces this Et group above the plane of the pyridine ring.

Finally, we sought to establish whether the high persistence of **17** translates to stable electrochemical cycling, a necessity for applications in RFBs. Thus, we subjected $\mathbf{17}^+$ to $1e^-$ charge−discharge cycling in a symmetric electrochemical cell and compared the results to those of $\mathbf{1}^+$, the progenitor of this study. Importantly, this experimental design was selected in order to isolate the charge−discharge reactions to those of the anolyte. This allows an evaluation of the anolyte's electrochemical cycling stability without complications that can arise in a complete redox flow battery (e.g., catholyte and membrane compatibility as well as crossover).[17] Galvanostatic cycling was performed on a 10 mM solution of $\mathbf{17}^+$ with reticulated vitreous carbon electrodes at 2.5C (Figure 5a). Upon the $1e^-$ reduction of $\mathbf{17}^+$ to **17**, an average state-of-charge of 95% was reached, and the anolyte discharged with 98% Coulombic efficiency (Figure 5b). No loss in storage capacity was observed for $\mathbf{17}^+$ after 200 cycles, and the cycling potentials are consistent with the redox potential measured by CV. These results are in marked contrast to cycling data for $\mathbf{1}^+$, which shows 35% capacity loss over the same time. The excellent cyclability of $\mathbf{17}^+$ at even lower potentials than the parent molecule $\mathbf{1}^+$ highlights the utility of this approach for ROM development/optimization.

In summary, we demonstrate that physical organic modeling of an organic electrolyte can deliver new ROMs that possess a previously elusive combination of properties for nonaqueous RFB applications. Importantly, although this approach was successfully demonstrated for the development of $\mathbf{17}^+$, it is not specific to this class of electrolyte. As such, we anticipate that it should prove more broadly applicable to the design and


DOI: 10.1021/jacs.7b00147
J. Am. Chem. Soc. XXXX, XXX, XXX−XXX

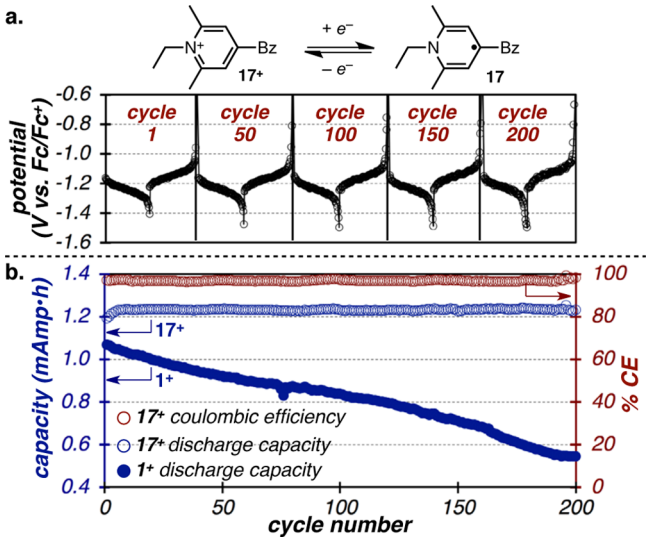


**Figure 5.** (a) Selected charge−discharge curves for the cycling of $\mathbf{17}^+$. (b) Comparison of cycling data for anolytes $\mathbf{1}^+$ and $\mathbf{17}^+$.

optimization of new ROM derivatives for applications in RFBs as well as in other electrochemical devices.

## ■ ASSOCIATED CONTENT

### Supporting Information

The Supporting Information is available free of charge on the ACS Publications website at DOI: 10.1021/jacs.7b00147.

Data for $C_{20}H_{18}NO$, $BF_4$ (CIF)
Data for $C_{20}H_{18}NO$ (CIF)
Experimental procedures, characterization, and spectral and electrochemical data (PDF)

## ■ AUTHOR INFORMATION


### Corresponding Authors

*mssanfor@umich.edu
*minteer@chem.utah.edu
*sigman@chem.utah.edu

### ORCID

Shelley D. Minteer: 0000-0002-5788-2249
Matthew S. Sigman: 0000-0002-5746-8830
Melanie S. Sanford: 0000-0001-9342-9436


### Notes

The authors declare no competing financial interest.

## ■ ACKNOWLEDGMENTS

This work was supported by the Joint Center for Energy Storage Research (JCESR) a Department of Energy, Energy Innovation Hub. We thank Dr. J. M. Kampf for X-ray crystallography, and the NSF (CHE-0840456) for X-ray instrumentation.

## ■ REFERENCES


(1) Gong, K.; Fang, Q.; Gu, S.; Li, S. F. Y.; Yan, Y. *Energy Environ. Sci.* **2015**, *8*, 3515.

(2) (a) Dunn, B.; Kamath, H.; Tarascon, J.-M. *Science* **2011**, *334*, 928. (b) Perry, M. L.; Weber, A. Z. *J. Electrochem. Soc.* **2016**, *163*, A5064.

(3) Darling, R. M.; Gallagher, K. G.; Kowalski, J. A.; Ha, S.; Brushett, F. R. *Energy Environ. Sci.* **2014**, *7*, 3459.

(4) (a) Soloveichik, G. L. *Chem. Rev.* **2015**, *115*, 11533. (b) Hicks, R. G. *Org. Biomol. Chem.* **2006**, *5*, 1321. (c) Chen, Z.; Qin, Y.; Amine, K. *Electrochim. Acta* **2009**, *54*, 5605. (d) Bockman, T. M.; Kochi, J. K. *J. Org. Chem.* **1990**, *55*, 4127. (e) Wei, X.; Cosimbescu, L.; Xu, W.; Hu, J. Z.; Vijayakumar, M.; Feng, J.; Hu, M. Y.; Deng, X.; Xiao, J.; Liu, J.; Sprenkle, V.; Wang, W. *Adv. Energy Mater.* **2015**, *5*, 1400678. (f) Assary, R. S.; Zhang, L.; Huang, J.; Curtiss, L. A. *J. Phys. Chem. C* **2016**, *120*, 14531. (g) Wei, X.; Xu, W.; Huang, J.; Zhang, L.; Walter, E.; Lawrence, C.; Vijayakumar, M.; Henderson, W. A.; Liu, T.; Cosimbescu, L.; Li, B.; Sprenkle, V.; Wang, W. *Angew. Chem., Int. Ed.* **2015**, *54*, 8684. (h) Brushett, F. R.; Vaughey, J. T.; Jansen, A. N. *Adv. Energy Mater.* **2012**, *2*, 1390. (i) Duan, W.; Vemuri, R. S.; Milshtein, J. D.; Laramie, S.; Dmello, R. D.; Huang, J.; Zhang, L.; Hu, D.; Vijayakumar, M.; Wang, W.; Liu, J.; Darling, R. M.; Thompson, L.; Smith, K.; Moore, J. S.; Brushett, F. R.; Wei, X. *J. Mater. Chem. A* **2016**, *4*, 5448. (j) Lin, K.; Chen, Q.; Gerhardt, M. R.; Tong, L.; Kim, S. B.; Eisenach, L.; Valle, A. W.; Hardee, D.; Gordon, R. G.; Aziz, M. J.; Marshak, M. P. *Science* **2015**, *349*, 1529.

(5) (a) Gerhardt, M. R.; Tong, L.; Gómez-Bombarelli, R.; Chen, Q.; Marshak, M. P.; Galvin, C. J.; Aspuru-Guzik, A.; Gordon, R. G.; Aziz, M. J. *Adv. Energy Mater.* **2016**, 1601488. (b) Weng, W.; Huang, J.; Shkrob, I. A.; Zhang, L.; Zhang, Z. *Adv. Energy Mater.* **2016**, *6*, 1600795. (c) Narayana, K. A.; Casselman, M. D.; Elliott, C. F.; Ergun, S.; Parkin, S. R.; Risko, C.; Odom, S. A. *ChemPhysChem* **2015**, *16*, 1179. (d) Chénard, E.; Sutrisno, A.; Zhu, L.; Assary, R. S.; Kowalski, J. A.; Barton, J. L.; Bertke, J. A.; Gray, D. L.; Brushett, F. R.; Curtiss, L. A.; Moore, J. S. *J. Phys. Chem. C* **2016**, *120*, 8461. (e) Carino, E. V.; Diesendruck, C. E.; Moore, J. S.; Curtiss, L. A.; Assary, R. S.; Brushett, F. R. *RSC Adv.* **2015**, *5*, 18822.

(6) Sevov, C. S.; Brooner, R. E. M.; Chénard, E.; Assary, R. S.; Moore, J. S.; Rodríguez-López, J.; Sanford, M. S. *J. Am. Chem. Soc.* **2015**, *137*, 14465.

(7) $\mathbf{1}^-$ and $\mathbf{1}^+$ persist as 0.70 M solutions for over 4 days.

(8) Verloop, A.; Tipker, J. *Pharmacochem. Libr.* **1977**, *2*, 63.

(9) (a) Sigman, M. S.; Harper, K. C.; Bess, E. N.; Milo, A. *Acc. Chem. Res.* **2016**, *49*, 1292. (b) Harper, K. C.; Bess, E. N.; Sigman, M. S. *Nat. Chem.* **2012**, *4*, 366.

(10) (a) Milo, A.; Neel, A. J.; Toste, F. D.; Sigman, M. S. *Science* **2015**, *347*, 737. (b) Niemeyer, Z. L.; Milo, A.; Hickey, D. P.; Sigman, M. S. *Nat. Chem.* **2016**, *8*, 610.

(11) Harper, K. C.; Vilardi, S. C.; Sigman, M. S. *J. Am. Chem. Soc.* **2013**, *135*, 2482.

(12) Consistent with decomposition by radical homocoupling, the immediate products could not be characterized as they react further to form intractable product mixtures.

(13) (a) Kosower, E. M.; Poziomek, E. J. *J. Am. Chem. Soc.* **1964**, *86*, 5515. (b) Itoh, M.; Nagakura, S. *Bull. Chem. Soc. Jpn.* **1966**, *39*, 369.

(14) (a) Huang, J.; Pan, B.; Duan, W.; Wei, X.; Assary, R. S.; Su, L.; Brushett, F. R.; Cheng, L.; Liao, C.; Ferrandon, M. S.; Wang, W.; Zhang, Z.; Burrell, A. K.; Curtiss, L. A.; Shkrob, I. A.; Moore, J. S.; Zhang, L. *Sci. Rep.* **2016**, *6*, 32102. (b) Schon, T. B.; McAllister, B. T.; Li, P.-F.; Seferos, D. S. *Chem. Soc. Rev.* **2016**, *45*, 6345.

(15) (a) Hermolin, J.; Levin, M.; Kosower, E. M. *J. Am. Chem. Soc.* **1981**, *103*, 4808. (b) Kosower, E. M. In *Preparative Organic Chemistry*; Springer: Berlin, Heidelberg, 1983; p 117.

(16) $\mathbf{17}^+$ has a solubilty of greater than 0.70 M in acetonitrile.

(17) (a) Montoto, E. C.; Nagarjuna, G.; Hui, J.; Burgess, M.; Sekerak, N. M.; Hernández-Burgos, K.; Wei, T.-S.; Kneer, M.; Grolman, J.; Cheng, K. J.; Lewis, J. A.; Moore, J. S.; Rodríguez-López, J. *J. Am. Chem. Soc.* **2016**, *138*, 13230. (b) Burgess, M.; Moore, J. S.; Rodriguez-Lopez, J. *Acc. Chem. Res.* **2016**, *49*, 2649. (c) Nagarjuna, G.; Hui, J.; Cheng, K. J.; Lichtenstein, T.; Shen, M.; Moore, J. S.; Rodríguez-López, J. *J. Am. Chem. Soc.* **2014**, *136*, 16309. (d) Liu, Y.; Lu, S.; Wang, H.; Yang, C.; Su, X.; Xiang, Y. *Adv. Energy Mater.* **2016**, 1601224. (e) Wild, A.; Strumpf, M.; Häupler, B.; Hager, M. D.; Schubert, U. S. *Adv. Energy Mater.* **2016**, 1601415. (f) Winsberg, J.; Hagemann, T.; Janoschka, T.; Hager, M. D.; Schubert, U. S. *Angew. Chem., Int. Ed.* **2017**, *56*, 686. (g) Janoschka, T.; Martin, N.; Hager, M. D.; Schubert, U. S. *Angew. Chem., Int. Ed.* **2016**, *55*, 14427. (h) Winsberg, J.; Stolze, C.; Muench, S.; Liedl, F.; Hager, M. D.; Schubert, U. S. *ACS Energy Lett.* **2016**, *1*, 976.




DOI: 10.1021/jacs.7b00147
J. Am. Chem. Soc. XXXX, XXX, XXX−XXX